



Exploring the correlation and synchronicity between environmental factors and occupant thermal response in dynamic outdoor cabin environments

Junmeng Lyu, Yuxin Yang, Dayi Lai, Li Lan, Zhiwei Lian^{*}

School of Design, Department of Architecture, Shanghai Jiao Tong University, Shanghai, China



ARTICLE INFO

Keywords:

Dynamic thermal responses
Facial skin temperature
Thermal sensation
Transient cabin environment
Solar radiation

ABSTRACT

To improve the cabin thermal environment and explore advanced automotive air-conditioning control methods, it is essential to understand the key factors affecting occupant thermal response as well as the synchronicity of the thermal response to environmental changes in outdoor conditions. Given the current gaps in research, this study conducted outdoor experiments in summer to analyze the correlation and synchronicity between the cabin thermal environment and occupant thermal sensation as well as facial skin temperature. Results showed that, during the cooling phases of experiments with high initial cabin air temperatures, occupant thermal sensation improved significantly within 7 min. After 15 min, facial skin temperature and thermal sensation reached quasi-steady states. Thermal sensation was primarily influenced by air temperature, followed by solar radiation, and exhibited significant synchronicity with changes in these factors. When the air temperature stabilized at around 26 °C, every 200 W/m² of solar radiation exposure increased the thermal sensation unit during the 40-min experiment period. Cheek and nose skin temperatures were significantly correlated with air temperature and solar radiation, and were sensitive to environmental changes, synchronizing with changes in air temperature and relative humidity. Further analysis showed the feasibility of using cheek and nose skin temperatures to characterize the occupant thermal sensation in a cabin. Additionally, this study found sex differences in the occupant thermal response in a cabin. The results provide insight into the key optimization parameters for comfort-oriented cabin thermal environment design and offer support for future air conditioning control in cabins based on thermal imaging.

Abbreviations

A/C	Air conditioner
T _{air}	Air temperature, °C
T ₀	Initial cabin air temperature, °C
T _{globe}	Globe temperature, °C
V _{air}	Air velocity, m/s
SR	Solar radiation, W/m ²
T _{air_re}	Air return temperature, °C
T _{air_su}	Air supply temperature, °C
T _{sur}	Surface temperature, °C
RH	Relative humidity, %
TSV	Thermal sensation vote
T _{sk}	Skin temperature, °C
LTSV	Local thermal sensation vote
SD	Standard deviation
T _{air_1.1m}	Air temperature at height of 1.1 m, °C
T _{air_0.1m}	Air temperature at height of 0.1 m, °C
T _{sur_ws}	Surface temperature of windshield, °C

(continued on next column)

(continued)

T _{sur_door}	Surface temperature of door, °C
T _{sur_window}	Surface temperature of window, °C
T _{sur_chair}	Surface temperature of seat back, °C
T _{sk}	Skin temperature, °C
dT _{sk} /dt	Skin temperature change rate, °C/s

1. Introduction

Vehicles are considered functional ‘compact built environments’ [1]. During warm conditions in summer, especially when entering the cabin, occupants may encounter extremely high-temperature environments, which not only affect comfort but also pose health risks such as heatstroke. With the advancement of automotive technology, particularly the transformation towards intelligence and electrification, the comfort of the cabin and thermal environment management have become

* Corresponding author.

E-mail address: zwlian@sjtu.edu.cn (Z. Lian).

important research topics.

Current research assessing thermal comfort in cabins often refers to the European standard EN ISO 14505 [2–4] and/or the American standard ASHRAE-55 [5]. These two standards use the Predicted Mean Vote (PMV-PPD) and Standard Effective Temperature (SET) to assess thermal comfort in cabins [2,3]. However, these assessment tools are designed for stable and uniform conditions in indoor environment of buildings. Conversely, the thermal environment in a cabin is significantly affected by frequently changing external conditions, compounded by the cabin's poor thermal insulation performance and extensive transparent enclosure structures, resulting in a thermal environment in the vehicle that is more complex than those in buildings and has a broader range of variations and more pronounced dynamics [6–8]. Grundstein et al. highlighted that, in summer, when the outdoor temperature is 34 °C and the solar radiation is approximately 800 W/m², the temperature inside a vehicle can reach up to 72 °C [9]. This leads to potentially significant differences in human skin heat dissipation and skin moisture levels in the cabin environment compared with those in a standard environment. Consequently, calculating the SET for this specific type of environment may not accurately represent the actual thermal sensations of individuals. The comparative study of evaluation indicators of Danca et al. underscores this issue [10]. Therefore, directly applying the results of thermal comfort research based on an indoor building environment to a cabin environment may not objectively describe the thermal comfort in this space.

Research on cabin thermal comfort has progressed significantly (Table 1). A series of experimental cabin studies conducted by Guan et al. explored human thermal response under conditions of rapid transient temperature changes and investigated methods for predicting human thermal sensation from an engineering application perspective [11,12]. Hodder et al. [13] studied the impact of solar radiation on passenger comfort by controlling the power of solar lamps in an experimental cabin. The correlation between solar radiation and thermal sensation of cabin occupants was also mentioned in the outdoor studies of Zhou et al. [6,8] and Srisilpsophon et al. [14]. A series of chamber studies conducted by Arens and Zhang et al. provided insights into the thermal responses of cabin occupants to air temperature changes and offered perspectives on the thermal response patterns and predictive models [15–18]. Kaynakli et al. and Kilic et al. conducted a series of field studies [19–23] to explore the characteristics of air velocity, air temperature, relative humidity, and surface temperature in the cabin during warming and cooling periods, and conducted questionnaires on the thermal sensations of subjects. Qi et al. [24] highlighted in their outdoor cabin study that assessments of occupant thermal sensation should consider the influences of position, body parts, and driving state. However, many studies, particularly those based on environmental simulation chambers settings, are often confined to specific quasi-steady states or environments in which a single variable can be controlled, and only a few studies explore human responses to transient conditions [25]. Such experiments conducted in environmental chambers allow for the control of the environmental chamber conditions, thereby facilitating the analysis of the impact of a single factor or those of various factors on human thermal sensation [26,27]. Nevertheless, when assessing thermal comfort in vehicles, it is necessary to consider that environmental characteristics exhibit strong transient parameters, both temporally and spatially [28], which are difficult to fully simulate in environmental chambers. Considering the potential for more complex variations in real-world cabin environments, some influencing factors identified in controlled experiments may be obscured by other variables owing to the combined effects of actual environmental factors. Related research has primarily focused on exploring factors related to human thermal sensation, including various surface structures and their temperatures, local changes in air temperature, air velocity distribution, relative humidity, solar radiation intensity, and clothing type [29]. However, the extents of the influences of different factors on human thermal sensation may vary significantly in real

Table 1
Studies related to cabin thermal comfort.

Ref	Subjects	Type	Environmental parameters	Thermal response
[11,12]	Not given (total of 16 tests)	Environmental chamber	T _{air} , T _{globe} , V _{air} , RH	T _{sk} , dT _{sk} /dt, Heat flux, Cumulative heat gain, TSV
[15–18]	27 subjects (15 females and 12 males)	Environmental chamber	T _{air} (both local and mean air temperatures)	TSV, LTSV, LTSV
[26]	15 male subjects	Environmental chamber	T _{air}	TSV, LTSV, T _{sk}
[13]	24 subjects	Environmental chamber	SR	TSV, T _{sk}
[31]	24 subjects	Outdoor & Environmental chamber	T _{air} , T _{air_re} , T _{air_su} , SR, V _{air} , T _{sur}	TSV
[6]	16 subjects (8 males and 8 females)	Outdoor (driving)	RH, T _{air} , T _{sur} , SR	TSV, T _{sk}
[7]	32 subjects (26 males and 6 females)	Outdoor (driving)	RH, T _{air} , T _{sur}	TSV, T _{sk}
[21]	Not given	Outdoor	RH, T _{air} , T _{sur}	TSV, T _{sk}
[24]	30 subjects (15 males and 15 females)	Outdoor	T _{air} , seat position	TSV, LTSV, T _{sk}

T_{air} = air temperature, °C.

T_{globe} = black globe temperature, °C.

T_{sur} = compartment interior surface temperature, °C.

T_{air_re} = air return temperature, °C.

T_{air_su} = air supply temperature, °C.

V_{air} = air velocity, m/s.

RH = relative humidity, %.

T_{sk} = skin temperature, °C.

dT_{sk}/dt = skin temperature change rate, °C/s.

Cumulative heat gain = change of mass averaged body temperature from the thermally neutral state, °C.

Heat flux = rate of heat transfer between the human body and its surroundings, W/m².

environments. Therefore, from the perspective of engineering optimization, it is necessary not only to focus on factors related to thermal sensation, but also to consider the extents of the impacts of different factors on human thermal sensation. By focusing on optimizing the key parameters in the thermal environment design, it is possible to maximize the marginal effects. Additionally, a study conducted in an underground parking area [30] indicated that the front row of a cabin reaches a quasi-steady-state thermal equilibrium within approximately 5–15 min under a single-zone air conditioning system. However, current research based on outdoor experiments still provides a limited understanding of the characteristics of changes in human thermal sensation during the dynamic cooling process, such as the environmental conditions and timing required to achieve a neutral state with air conditioning in real environments. Thorough exploration of the response patterns of thermal sensation to environmental changes is crucial for guiding the intelligent pre-cooling design of vehicle cabins, which can not only enhance occupant comfort, but also effectively decrease heat stress risks in high-temperature climates.

Skin temperature serves as a physiological indicator of human thermal response and establishes an intermediary between the environment and perception. Understanding the reaction of skin temperature to environmental conditions enables a more accurate assessment of the level of occupant thermal sensation. The application of skin

temperature to the design and control parameters of cabin air-conditioning systems may represent a new pathway for developing air-conditioning systems that balance comfort and energy efficiency. In the field of indoor building environments, environmental control based on skin temperature is feasible [32]. However, in the context of vehicle cabins, from a safety perspective, the premise for environmental control based on skin temperature data is that the temperature measurement process should be low-interference and non-contact. The use of thermal imaging sensors for non-contact measurement of skin temperature has emerged as a research hotspot in the field of thermal comfort [33–37]. Among these, the face has garnered widespread attention owing to its prolonged exposure to the environment, and some studies have demonstrated that its temperature variation characteristics are correlated with thermal sensation [35,37,38]. However, studies on facial skin temperature variability patterns primarily focus on indoor building environments and are often based on data from chamber experiments in steady-state environments. In contrast, the thermal environment of a cabin is characterized by complexity and rapid adjustability, which may result in a different relationship between facial skin temperature and the environment. Taniguchi et al. [39,40] studied the effect of cold air on facial skin temperature in a simulated cabin environment and found that during the cooling process of the cabin under constant solar radiation intensity, facial skin temperature and its change have specific patterns. However, in a comprehensive environment, the factors influencing facial skin temperature and the extent of their impacts require further clarification. Moreover, current research on skin temperature has largely demonstrated its correlation with environmental parameters. However, whether facial skin temperature can respond synchronously to cabin environment changes—that is, whether the response characteristics of facial skin temperature can match the characteristics of environmental changes—is a prerequisite for using it for environmental control. The rapid adjustment of the cabin thermal environment and its complex variability in real scenarios impose higher demands on the synchronicity of facial skin temperature response. Whether facial skin temperature can respond to dynamic changes of the cabin thermal environment in real scenarios needs to be assessed. Furthermore, owing to variations in the distribution of facial fat and cartilage, sensitivity to temperature changes may also differ across different regions. Identifying the regions most sensitive to changes in the cabin environment could provide valuable guidance for the selection of temperature extraction locations in thermal imaging applications and may have implications for the design of intelligent air-conditioning control systems.

To address these limitations, we conducted an experiment in an outdoor cabin. A series of dynamic thermal environments were created inside the cabin, and environmental parameters, including solar radiation, indoor air temperature, indoor surface temperature, and relative humidity, were recorded in real time. The subjective thermal sensations of the participants throughout the experiment were collected through questionnaires, and their facial skin temperatures were captured using an infrared thermal imager. This study focused on the following objectives:

(1) The characteristics of cabin thermal environment changes and human thermal responses after the activation of the car A/C under real-world conditions were investigated. (2) Based on real-world data, the significant factors affecting human thermal response (including thermal sensation and facial skin temperature) and the extents of their impacts were analyzed. (3) The synchronicity between changes in the temperature of different facial regions and thermal environment parameters after the activation of the car A/C were assessed. (4) The correlation between human thermal sensation and facial skin temperature in the cabin environment was explored.

2. Method

2.1. Experimental conditions

This study conducted experiments to investigate the thermal sensation of individuals and the characteristics of facial skin temperature changes in a vehicle cabin. The experiments were conducted in a vehicle parked outdoors at Shanghai Jiao Tong University from July to August 2023.

Cabin environments differ from indoor building environments. When a vehicle is parked under sunlight, the air temperature inside the cabin can become extremely high, with the occupants being immediately exposed to extremely high initial cabin air temperatures upon entering the vehicle. During preliminary experiments conducted in a vehicle parked outdoors in Shanghai in summer under direct sunlight, we monitored the cabin air temperature. The results showed that after prolonged exposure, the cabin air temperature could generally rise to 55 °C and occasionally reach approximately 60 °C. In this study, initial cabin air temperatures (T_0) of 55, 45, and 35 °C were selected as the conditions for participant entry during daytime. The temperature of 55 °C represents the high-temperature condition achieved after prolonged exposure, 45 °C is utilized to simulate a more typical high-temperature cabin environment, and 35 °C is indicative of the cabin conditions following short-term exposure to sunlight during daytime. In the absence of sunlight during the evenings, the cabin air temperature when parked outdoors was approximately 30 °C. This temperature was used as the baseline condition for comparison. This setup was designed to cover various possible initial cabin thermal conditions, allowing for a more comprehensive assessment of the impact of the cabin environment on occupants. To ensure that the initial cabin air temperature to which the participants were exposed under the experimental conditions met the designed values, we implemented a comprehensive strategy for controlling the initial temperature conditions within the cabin. By adjusting the duration of the vehicle's exposure to sunlight and employing thermocouples for continuous real-time monitoring of the cabin air temperature, we could accurately track the temperature changes within the cabin in real time. When the monitored temperature approached the designed initial value, the participants were transferred from the adaptation room to the cabin to commence the experiment. Furthermore, to investigate whether there were differences in thermal sensation and facial skin temperature characteristics between situations with direct sunlight on the front windshield and situations with sunlight entering the cabin from the side, the orientation of the vehicle was adjusted to create different conditions (see Fig. 1). Each experimental session involved two participants simultaneously as well as a research team member conducting operations within the cabin. Each participant was assigned a fixed seat number and was required to maintain this seat throughout all subsequent experimental conditions. Because there was no sunlight during nighttime, each participant only participated in one nighttime condition (with two participants sitting in the front row seats). The experiment employed a full factorial experimental design requiring the participants to engage in combinations of various initial cabin air temperatures and vehicle orientations (see Table 2). Each participant completed seven experiments.

Each participant was exposed to various solar radiation intensities to cover a broad range of solar radiation levels within the experimental sample. Daytime experiments were conducted under clear weather conditions between 9:00 and 17:00. The participants were required to engage in two trials (one for each vehicle orientation) during each of the morning (9:00–11:00), noon (12:00–14:00), and afternoon (15:00–17:00) sessions. The sequence of experimental conditions for each participant was randomized to mitigate the collinearity between the initial cabin air temperature and solar radiation intensity. In each experimental condition, once participants entered the vehicle cabin and completed the initial questionnaire, the A/C was activated and set to “cooling + recirculation” mode. By adjusting the A/C set point, the cabin

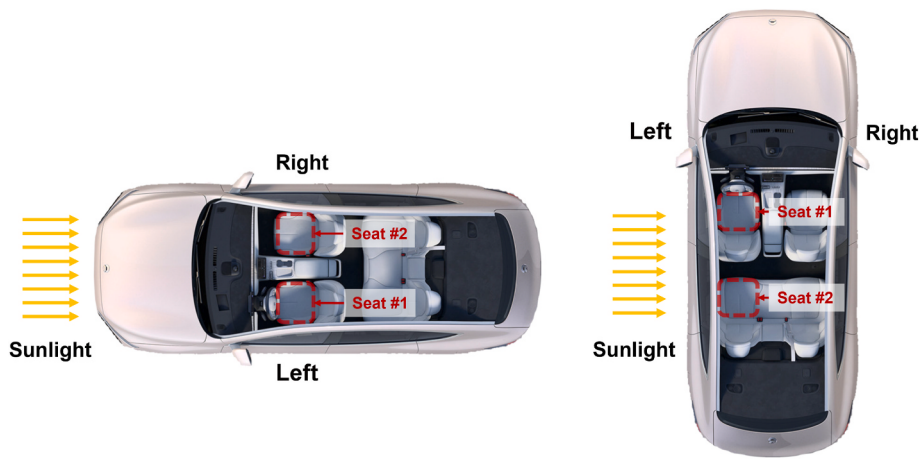


Fig. 1. Schematic diagram of the direction of sunlight incidence.

Table 2
Experimental conditions.

Condition	Initial cabin air temperature (°C)		Sunlight incidence direction
	Designed	Measured	
C1	55	53.6 ± 1.6	Frontal
C2	45	46.6 ± 1.7	
C3	35	36.9 ± 2.1	
C4	55	54.1 ± 2.8	Lateral
C5	45	42.7 ± 1.9	
C6	35	37.2 ± 1.4	
C7	30	30.7 ± 1.3	(Nighttime)

air temperature was stabilized at 25.5 ± 1.0 °C, within the neutral temperature range defined by ASHRAE-55 [41]. Furthermore, considering the limited space within the cabin and the proximity of occupants to the A/C vents, the angle of the vents was horizontally adjusted to 75° upward to prevent occupant discomfort caused by direct exposure to cold air from the vents. Throughout the experimental sessions, the doors and windows of the vehicle remained closed. Additionally, in all experiments, the sunroof and its shade were kept closed to mitigate any potential influence of the transparent sunroof on the experimental results. Appendix Table S1 lists the outdoor environmental parameters used in the experiments. During the daytime experiments, the outdoor air temperature and relative humidity remained relatively stable and consistent; during the nighttime experiment, the outdoor air temperature outside the vehicle was relatively low (30.0 ± 0.3 °C).

2.2. Experimental procedure

EN ISO 14505 specifies that automotive thermal comfort experiments should involve at least eight participants. In this study, the participant sample size was calculated strictly according to the G*Power software, and the F-test (linear multiple regression: fixed model, R^2 increases) was selected as the statistical test. The effect size was set to 0.15 (medium effect size), α error was set to 0.05, $1-\beta$ error was set to 0.80, and number of predictors was set to 5 [42]. The calculated minimum sample size was 92. As each participant participated in experiments under seven different conditions, the calculated minimum number of participants was 14. Finally, a sample size of 24 was chosen (12 males and 12 females). The participants included both college students and staff, and their information is provided in Table 3. All participants signed informed consent forms, refrained from consuming caffeine and alcohol and engaged in vigorous physical activity prior to the experiment. During the experiment, female participants wore clothing with a thermal insulation of approximately 0.51 clo, whereas male participants wore clothing with a thermal insulation of approximately 0.45 clo.

Table 3
Participant information.

	Number	Age	Height (cm)	Weight (kg)
Male	12	23.2 ± 1.6	173.5 ± 5.1	64.5 ± 6.8
Female	12	24.4 ± 2.1	163.5 ± 5.5	54.1 ± 4.8

Detailed clothing information is listed in Appendix Tables S2 and S3. This study was approved by the Ethics Committee of Shanghai Jiao Tong University.

As shown in Fig. 2, the total duration of each experiment was at least 62 min, including a minimum of 20 min for pre-experimental adaptation, a 2-min transition period from outdoors to the cabin, and a subsequent 40-min formal experiment inside the cabin. During the adaptation period, participants stayed in a room with a controlled temperature of 26 °C and air velocity lower than 0.2 m/s to eliminate any prior thermal experiences. Upon initiation of the formal experiment, the participants entered the cabin and completed an initial questionnaire (refer to Appendix Fig. S1), after which facial imaging was conducted. Subsequently, A/C was immediately activated. Throughout the experiment, participants completed thermal sensation questionnaires and underwent facial thermal imaging at fixed time intervals. The participants remained seated throughout the experiment for safety reasons and were not in a driving state.

2.3. Experimental measurements

During the experiment, the air and surface temperatures within the cabin were continuously recorded using a thermocouple system. Because of their potentially slow responses (generally longer than 5 min [43]), black globe thermometers would not have been able to reflect instantly and accurately the temperature changes that occur rapidly upon the activation of the cabin A/C. Therefore, black globe temperature measurements were not included in the experiments [44,45]. The specific measurement locations and descriptions are presented in Appendix Fig. S2 and Appendix Table S4. Two thermocouples were affixed approximately 0.1 m in front of the occupants' head and employed to collect real-time air temperature data at the location of the head exposure (P12–P14). A solar radiometer with an accuracy of ± 5 W/m² or ± 5 % of readings was horizontally positioned atop the instrument cluster to continuously collect total solar radiation data within the vehicle interior. The monitoring point for the outdoor environmental parameters was located 2 m outside the cabin, providing real-time measurements of air temperature, solar radiation, and relative humidity. Details on the measuring instruments are listed in Appendix Table S5. For more details about the experiment, please refer to the published study [46].

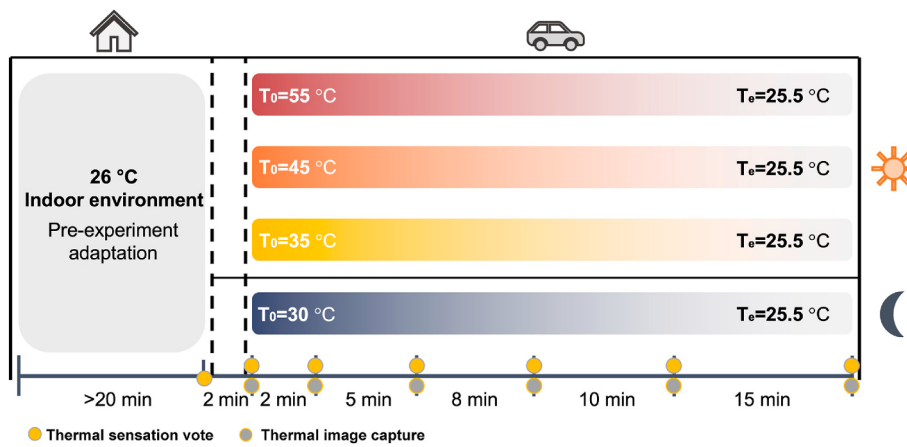


Fig. 2. Experiment procedure.

For skin temperature measurements, this study used high-performance infrared thermography (FLIR T-460, FLIR Systems Inc, USA) with a resolution of 320×240 pixels and an accuracy of $\pm 1\text{ }^\circ\text{C}$ or $\pm 1\%$ of readings. The infrared thermography was factory-calibrated to acquire accurate measurements. In addition, the thermography performed automatically flat-field calibration when the sensor temperature changed to compensate for the effects of reading drift. Temperature extraction was performed using the FLIR Thermal Studio software. The infrared emissivity of the human surface was set to 0.98, which is appropriate for human skin [33]. The reflected and atmospheric temperatures were set to the air temperature at 1.1 m height collected by the thermocouple. To validate the accuracy of the infrared thermography used in this study, an independent validation experiment was conducted to compare the infrared thermography and PyroButton readings [37]. The latter instrument has been proven to be reliable for measuring skin temperature. The difference in readings between FLIR T-460 and Pyro-Button for facial skin temperature acquisition in indoor environments between 23 and 30 $^\circ\text{C}$ was found to be less than 0.3 $^\circ\text{C}$. For details on the validation, we refer to our previous study [37]. In addition, because of the limitations imposed by the field of view of the infrared thermography, the thermography was not mounted in a fixed manner inside the vehicle. To ensure the capture of comprehensive facial thermal imaging data, imaging was conducted manually by a member of the research team seated in the cabin. The members involved in this procedure were specifically trained to standardize the imaging process. Strict control over the imaging distance was maintained throughout the experiment, with the thermography consistently positioned 0.5 m away from the participants. This distance was determined based on the required resolution and image quality. A detailed imaging perspective and the data collection region are presented in Appendix Fig. S3.

2.4. Statistical analysis

2.4.1. Correlation analysis between thermal response and environment

The quantitative relationships between variables were analyzed using a generalized linear mixed model (GLMM). This approach is useful for incorporating continuous and categorical predictors. When the predictors are continuous, they are treated as fixed effects, and their coefficients represent the correlation between the dependent variable and the predictors, holding all other variables constant. Categorical predictors are included in the model as fixed effects using dummy coding or other coding schemes. The coefficients of the categorical variables represent the response variable differences for different categorical variable levels relative to the reference category. The coefficients of the other categorical variable levels represent the expected response variable differences relative to the reference category.

2.4.2. Analysis of the synchronicity between thermal response and environmental changes

In stable environments, the sensitivity of the thermal responses to environmental changes can be assessed by evaluating the coefficients obtained from the regression of two sets of raw data. However, in dynamic environments, analyzing the synchronicity of changes between two variables (i.e., the sensitivity of one variable's response to another) becomes more complex. In such environments, both human thermal responses and environmental parameters change over time, as indicated by Variables #1 and #2 in Fig. 3. When conducting a bivariate regression analysis (R1) on the two variables over time, as well as a regression analysis (R2) on the changes in these variables over time ($\Delta(\text{Variable } \#1)$ and $\Delta(\text{Variable } \#2)$), four outcomes may arise: (1) both R1 and R2 are statistically significant; (2) only R1 is statistically significant, whereas R2 is not; (3) only R2 is statistically significant, whereas R1 is not; and (4) both R1 and R2 are statistically insignificant. The fourth scenario indicates no correlation between the two variables. The data distribution diagrams for the first three scenarios are shown in Fig. 3, representing the possible situations that may occur.

- (1) Both R1 and R2 are significant (Fig. 3(a)): The significance of R1 indicates a correlation between Variable #1 and Variable #2, meaning that when Variable #1 increases, Variable #2 also increases. The significance of R2 indicates that the changes between the two over time are synchronous. As shown in Fig. 3(a2), when Variable #1 changes rapidly, Variable #2 responds rapidly, and when the change in Variable #1 is slow, the change in Variable #2 also diminishes.
- (2) R1 is significant, whereas R2 is not (Fig. 3(b)): When both variables decrease over time, R1 is significant because a smaller Variable #1 corresponds to a smaller Variable #2, indicating their correlation. However, the lack of significance in R2 suggests that their changes are not synchronized; that is, Variable #2 does not respond quickly when Variable #1 changes rapidly. In this scenario, $\Delta(\text{Variable } \#2)$ might remain constant, leading to the R2 not being statistically significant. This result, in contrast to point (1), proves the necessity of conducting a second type of regression in environments with monotonic dynamic change, in which if both R1 and R2 are significant, Variable #2 is sensitive to changes in Variable #1.
- (3) R1 is not significant, whereas R2 is (Fig. 3(c)): In cases where the change in Variable #1 is very sharp, leading to a distribution of data as that in Fig. 3(c2), with data being overly concentrated on the smaller side of Variable #1, there is a weak correlation between the two variables. However, regressing $\Delta(\text{Variable } \#1)$ and $\Delta(\text{Variable } \#2)$ captures some aspects of their synchronicity in changes over time. This indicates that when using regression to

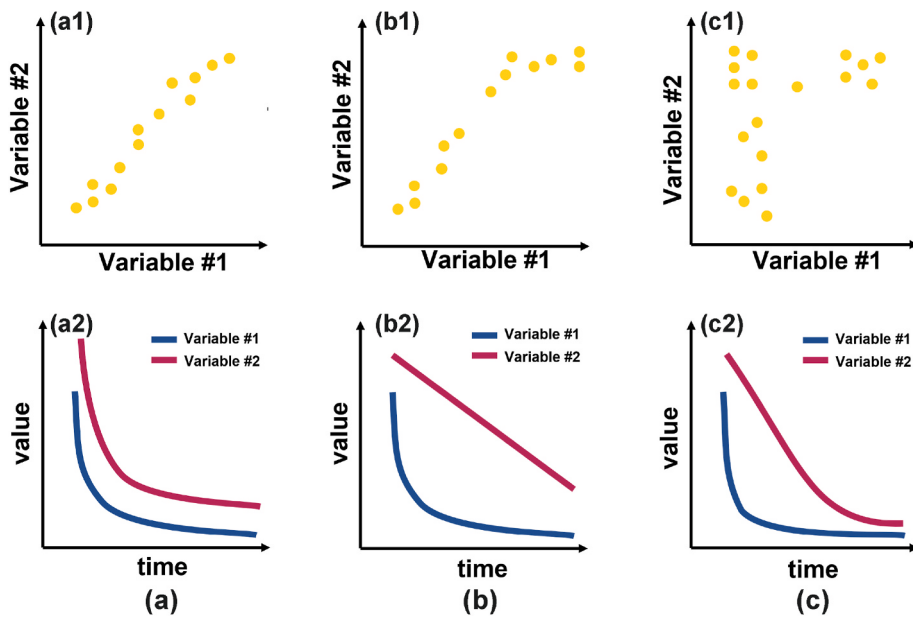


Fig. 3. Schematic diagram of the three relationships between two time-varying variables.

analyze the relationship between two variables, the relationship between the changes of each variable over time (i.e., $\Delta(\text{Variable } \#1)$ and $\Delta(\text{Variable } \#2)$) should be considered to analyze the synchronicity of the changes between the two variables or the sensitivity of the dependent variable to the changes in the independent variable. Conducting a regression analysis solely on the raw data of the two variables can prove the existence of a correlation between them; however, it cannot demonstrate whether these changes are synchronized.

Statistical significance was set to $P < 0.05$. In this study, one asterisk signifies a significant difference at $P < 0.05$, whereas two asterisks signify a highly significant difference at $P < 0.01$. All data were statistically analyzed using the SPSS software (version 26.0; SPSS, Inc., Chicago, IL, USA).

3. Results

3.1. Dynamic cabin environment characteristics

Fig. 4 depicts the variations in air supply temperature under four different initial cabin air temperature conditions ($55, 45, 35$, and 30°C). Detailed air supply temperature data, distinguished by the direction of solar incidence and vents, are available in Appendix Table S6. Within the initial 10 min after activating the A/C, the air supply temperature decreased rapidly. After the first 10 min, the air supply temperature stabilized at approximately $8\text{--}10^\circ\text{C}$ and remained constant until the completion of each session.

Fig. 5 shows the near-head region air temperatures under four different conditions. In cabins with initial air temperatures of 45 and 55°C , the air temperature experienced a rapid decline within the initial 15 min following the activation of the A/C, and the air temperature reached relative stability after 20 min. In the case of a cabin with an initial air temperature of 35°C , the cabin air temperature stabilized within approximately 10 min of activating the A/C. This shorter

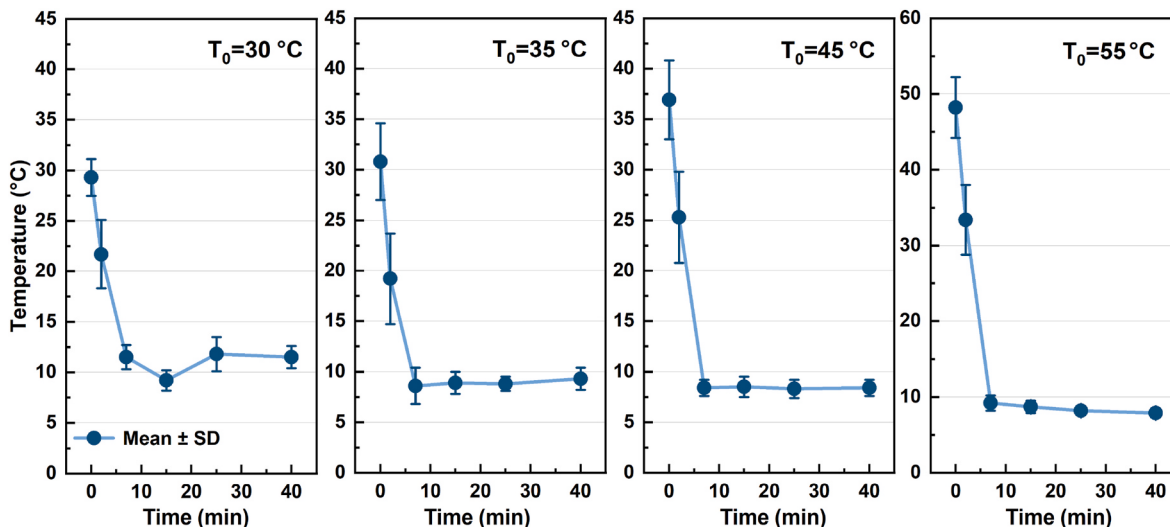


Fig. 4. Air supply temperature monitoring in the vent during the experimental period.

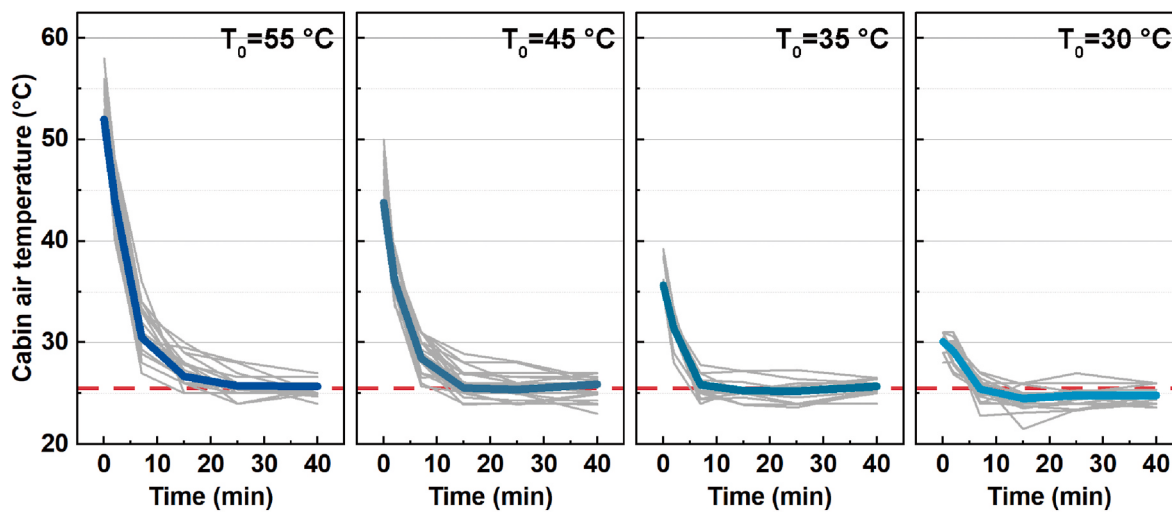


Fig. 5. Air temperature in occupant breathing zone during the experimental period.

stabilization time can be attributed to the nighttime experimental conditions, which lacked solar radiation, and the fact that the initial temperature was closer to the neutral range.

Fig. 6 illustrates the variations in cabin relative humidity across the four initial cabin air temperatures. Detailed data on the relative humidity, distinguished by the direction of solar incidence, are available in Appendix Table S7. Apart from the nighttime experimental group, where the vehicle's interior relative humidity was slightly higher, the remaining (daytime) experiments demonstrated that upon activation of the A/C, the cabin's relative humidity rapidly decreased and stabilized within 7 min of activation, with an average of approximately 30 %. Appendix Table S8 presents the solar radiation values incident on the glass under the experimental conditions.

The internal surface temperatures of the cabin under various experimental conditions were statistically analyzed, and the detailed data are presented in Appendix Table S9. During daytime, the surface temperature of the cabin's top sunroof can exceed 60 °C. The front windshield and side windows, characterized by the low thermal inertia of glass, maintain internal surface temperatures above 30 °C even after the cabin air temperature stabilizes. The inner surface temperature of the car doors can decrease and stabilize with decreasing air temperature. Additionally, considering the internal surface temperatures and solar radiation entering the cabin during experiments with frontal solar

incidence experienced by subjects 5 and 6 as an example (see Appendix Fig. S4), rapid changes in solar radiation can lead to significant variations in the temperatures of transparent surfaces exposed to sunlight, such as windshields and car windows.

Spearman's correlation analysis was conducted across the entire dataset to examine the relationships between environmental parameters. The calculated correlation coefficients are presented in Fig. 7. No significant differences were observed in the environmental conditions experienced by participants in different seating positions. In terms of air temperature, a strong correlation was found between air temperatures at heights of 1.1 and 0.1 m ($R = 0.84$). Solar radiation intensity was not significantly correlated with air supply temperature. The correlations between different surface temperatures were generally high, particularly between the inner surface temperatures of the car door, windshield, and side windows, with correlation coefficients ranging from 0.80 to 0.97. Additionally, a Spearman's correlation analysis was conducted between the "sex" variable and environmental parameter variables. The results indicated no significant differences in the environmental conditions experienced by participants of different sexes (correlation coefficient: 0.00–0.15; no significance). Given the collinearity and controlled variables in the study, a subsequent, more in-depth analysis was conducted to assess the influences of "T_{air_1.1m}", "SR", "RH", "sex", and "orientation" on the thermal responses of cabin

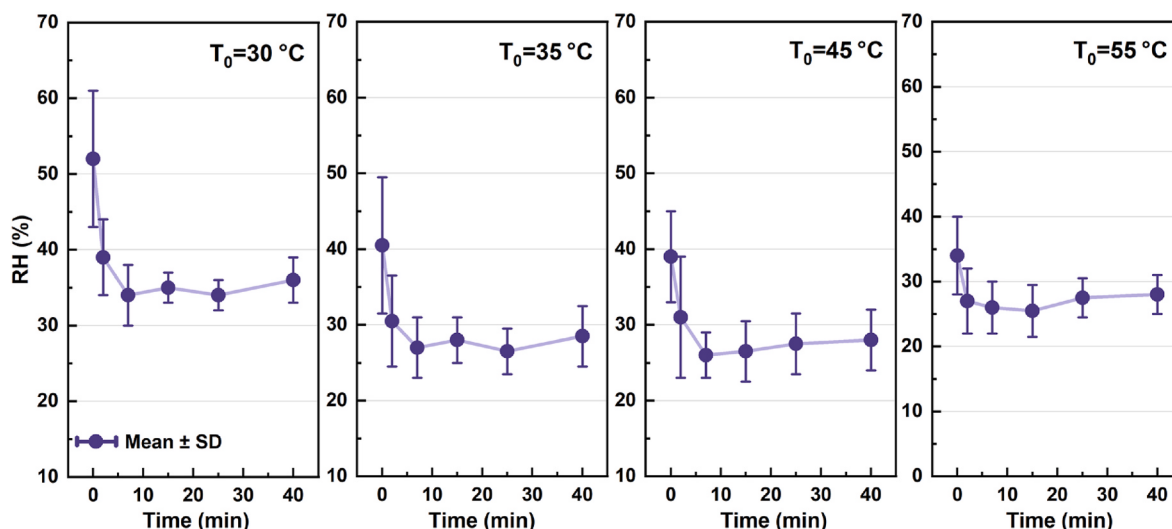


Fig. 6. Relative humidity monitoring during the experimental period.

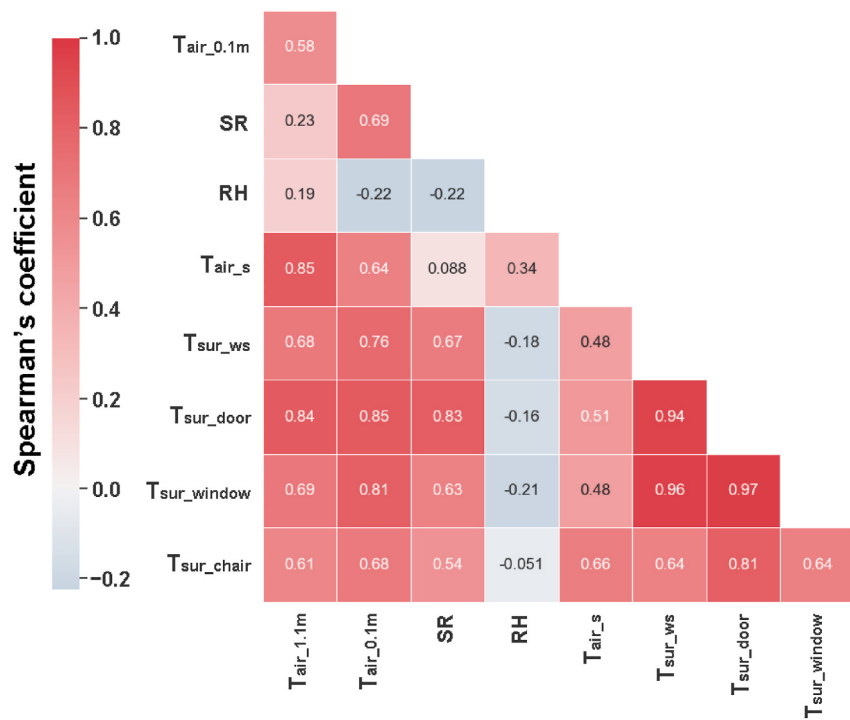


Fig. 7. Correlation heatmap of environment variables.

occupants.

3.2. Overall thermal sensation

Fig. 8 illustrates the variation in occupant thermal sensation under

four different initial cabin air temperature conditions (55, 45, 35, and 30 °C). When occupants entered cabins with initial air temperatures of 45 and 55 °C, their immediate thermal sensations could exceed 2.5. Over time, there was an improvement in occupant thermal sensation. The most significant change in thermal sensation occurred during the first

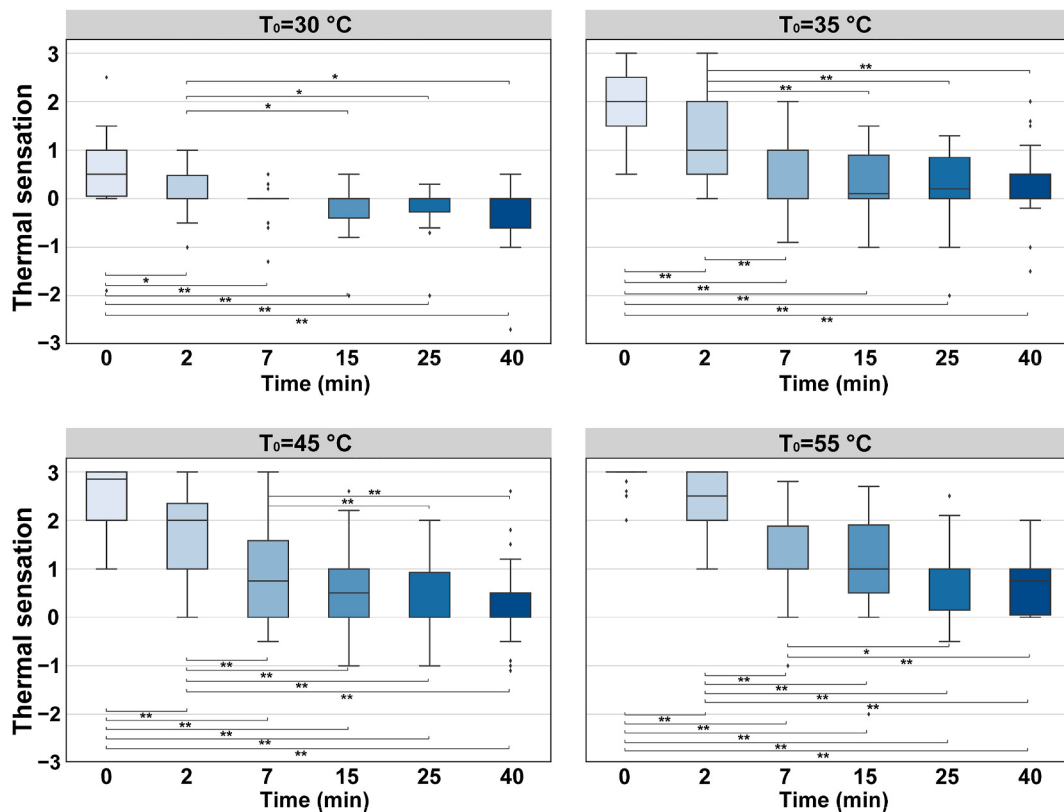


Fig. 8. Dynamic changes of occupant thermal sensation.

2–7 min after occupants entered the cabin. Between the 7th and 15th minutes, occupant thermal sensation dropped significantly below 1.0. Beyond the 15th minute, occupant thermal sensation was nearly.

A GLMM was employed to analyze the factors influencing occupant thermal sensation. The corresponding coefficients from the model are shown in Fig. 9. Concerning the overall thermal sensation, no significant difference was observed between front-seat occupants when direct sunlight illuminated the front windshield and occupants on the left side of the cabin (including both the first and second rows) when sunlight entered the cabin from the left side. There were significant positive correlations between occupant thermal sensation and both air temperature and solar radiation intensity ($P < 0.05$). Notably, the overall thermal sensation votes revealed significant sex differences ($P = 0.035$), with male participants reporting significantly higher thermal sensation votes than female participants. This finding is consistent with those of several previous studies conducted in indoor building environments [47–49]. Relevant research has indicated that sex differences in thermal sensation are less pronounced in warmer environments. However, in neutral and cooler environments, males tend to experience warmer than females.

Further analysis of the statistical relationships between changes in environmental parameters and thermal sensation was conducted using multiple regression models. The regression coefficients reflect the synchronicity of changes in thermal sensation in response to changes in environmental parameters (i.e., solar radiation, air temperature, and relative humidity). The analytical results are listed in Table 4. The results indicate that, for males, thermal sensation is significantly sensitive to changes in air temperature, relative humidity, and solar radiation, indicating that thermal sensation changes are synchronized with these environmental parameters, with the highest synchronicity observed in response to air temperature changes. For females, thermal sensation is significantly sensitive to changes in air temperature and solar radiation.

Fig. 10 depicts the relationship between steady-state thermal sensation and solar radiation. Thermal sensation increases by approximately 1 unit for every 200 W/m^2 increase in solar radiation intensity transmitted through the cabin window. Solar radiation is classified into four levels, namely A, B, C, and D, corresponding to intervals of 0, (0, 150], (150, 300], and (300, 450] W/m^2 , respectively. Occupant thermal sensation corresponding to each category is shown in Fig. 10(b). Under the Level B solar radiation range, occupant thermal sensation is not significantly different from that without solar radiation ($P > 0.05$). This suggests that solar radiation at this level has a relatively minor impact on occupant thermal sensation. However, as solar radiation reaches higher levels, such as Levels C and D, individuals distinctly perceive the thermal sensation gains it imparts ($P < 0.01$).

Variable		Coef.	Sig.
Orientation	Frontal	-0.053	0.259
	Lateral	Reference level	
Sex	Male	+0.097	0.035
	Female	Reference level	
Air temperature		+0.093	<0.001
Solar radiation		+0.002	<0.001
Relative humidity		-0.004	0.254

Fig. 9. Generalized linear mixed model regression results of occupant overall thermal sensation in relation to various factors.

Table 4

Multivariate regression results of thermal sensation variations with solar radiation, air temperature, and relative humidity variations.

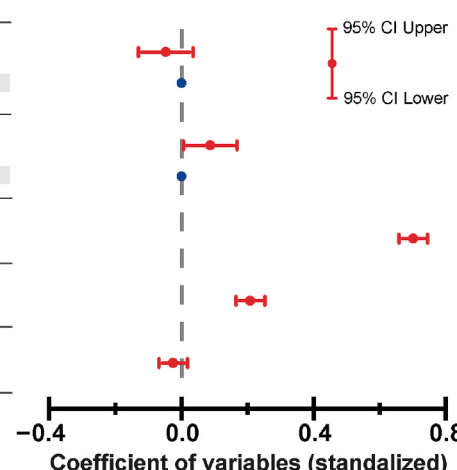
Sex	Variables	Unstandardized coefficients		Standardized coefficients	Sig.
		Coefficients	Std. error		
Male	ΔSR	+0.001	0.000	+0.167	0.000
	$\Delta T_{air,1.1m}$	+0.071	+0.006	+0.509	0.000
	ΔRH	+0.011	+0.004	+0.103	0.014
Female	ΔSR	+0.001	0.000	+0.093	0.046
	$\Delta T_{air,1.1m}$	+0.071	+0.008	+0.428	0.000
	ΔRH	+0.002	+0.005	+0.015	0.748

3.3. Local thermal sensations

The statistical values of the local thermal sensation votes at different time intervals are listed in Appendix Table S10. The sudden exposure of occupants to high temperatures can lead to elevated local thermal sensations throughout the body. However, as the cabin A/C is activated and the air temperature begins to change dynamically, the local thermal sensations improve in most body regions within 15 min. Because the seat surface fits on the occupant's back, it cannot cool down effectively, resulting in the local thermal sensation vote for the back being consistently higher than 1.0 (slightly warm). Fig. 11 illustrates the relationship between the local thermal sensations and solar radiation intensity at the 40th minute. When sunlight directly hits the windshield, the local thermal sensations of the forearms and thighs exhibit a stronger correlation with solar radiation intensity than those of other body regions, primarily owing to the direct influence of sunlight ($R = 0.412$; $P < 0.01$). In cases where sunlight enters the cabin from the side, the local thermal sensations in specific body parts (face, forearm, upper arm, thigh, and calf) on the windowed side are significantly higher than those on the non-windowed side ($P < 0.05$).

3.4. Facial skin temperature

Fig. 12 shows the variations in facial skin temperature of occupants under the four initial cabin air temperature conditions. When occupants entered a cabin with a temperature of 55°C , their facial skin temperature rose significantly. The nose region exhibited the highest mean temperature (38.9°C for males and 38.7°C for females), followed by that of the forehead region (38.4°C for males and 38.5°C for females). Facial skin temperatures gradually decreased with increasing cabin occupancy duration. After 15 min of being inside the cabin, facial skin



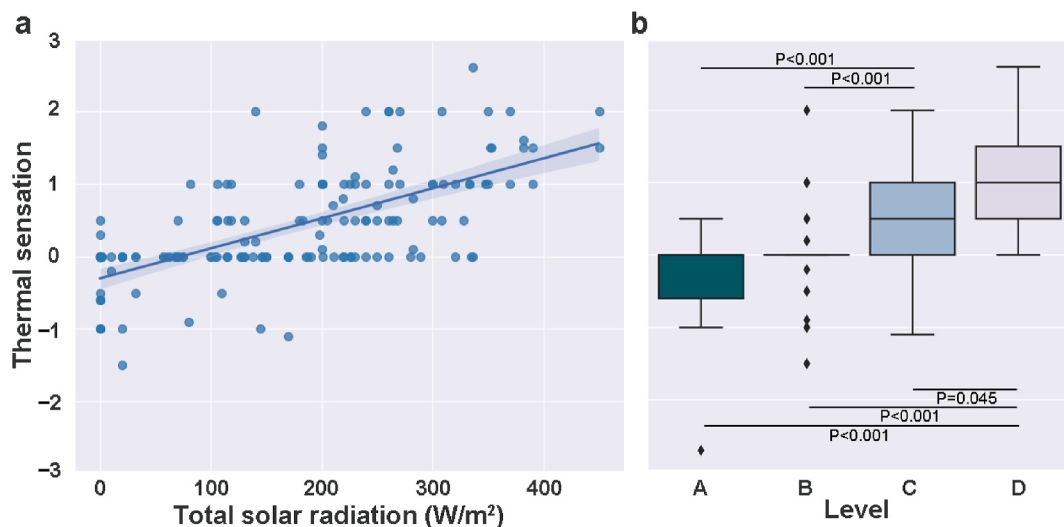


Fig. 10. Effects of solar radiation on steady-state overall thermal sensation.

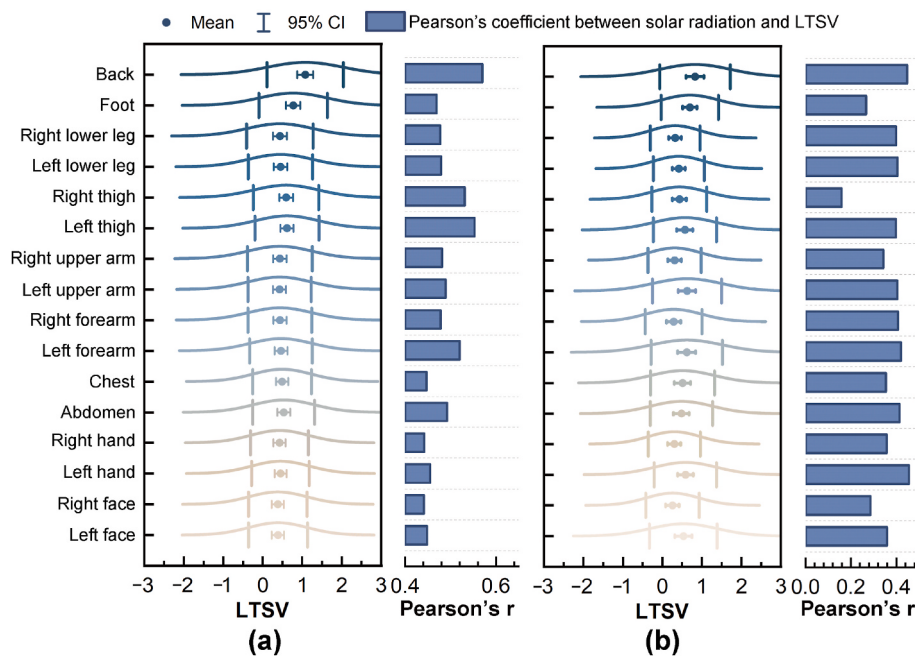


Fig. 11. Local thermal sensations under steady state and correlations with solar radiation.
(a) frontal sunlight; (b) lateral sunlight.

temperatures stabilized. Notably, when cabin air temperature stabilized at 25.5 °C, occupants in daytime experiments had higher facial skin temperatures compared to those in nighttime experiments. The most significant temperature difference was found in the cheek region, with differences exceeding 0.7 °C.

Notable differences in facial skin temperature distribution between males and females were also observed. Females exhibited a more pronounced non-uniform distribution of facial skin temperatures, particularly during the nighttime experiment and beyond the 25th minute in daytime experiments. During the nighttime experiment, after the facial skin temperatures of the occupants had stabilized, the temperature range among different facial regions was approximately 0.8 °C for males, whereas for females, it could exceed 2 °C. Among the facial regions, the cheeks exhibited the lowest temperature, whereas the forehead exhibited the highest temperature. Under the daytime experimental conditions, the maximum difference in facial skin

temperature non-uniformity between males and females was approximately 1 °C.

Factors affecting the skin temperature of multiple facial regions were analyzed using a GLMM model. The obtained correlation coefficients are shown in Fig. 13. Overall, there were significant correlations between facial skin temperature and both air temperature and solar radiation intensity. Specifically, for different facial regions, higher air temperatures and solar radiation were associated with higher cheek and nose skin temperatures ($P < 0.001$). When the cabin was subjected to lateral solar radiation, no significant difference was observed in the cheek skin temperatures of individuals near the window compared with those when the occupants were under frontal solar radiation ($P = 0.292$). Conversely, when the occupants were exposed to frontal solar radiation, the cheek skin temperatures on the side not adjacent to the window were significantly higher than those during exposure to lateral solar radiation ($P < 0.001$). The potential cause for the uneven temperature distribution

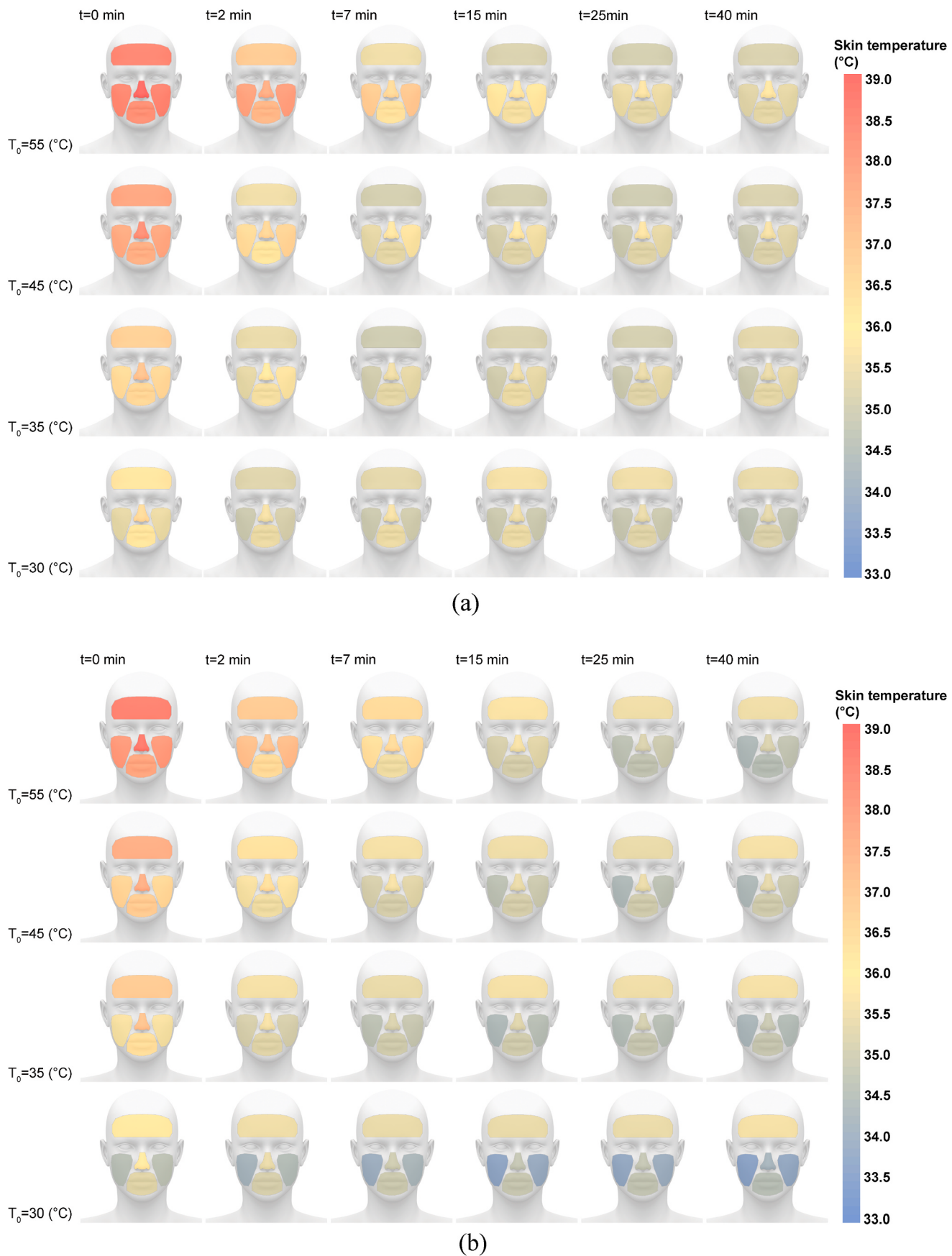


Fig. 12. Dynamic changes of facial skin temperature. (a) male (b) female.

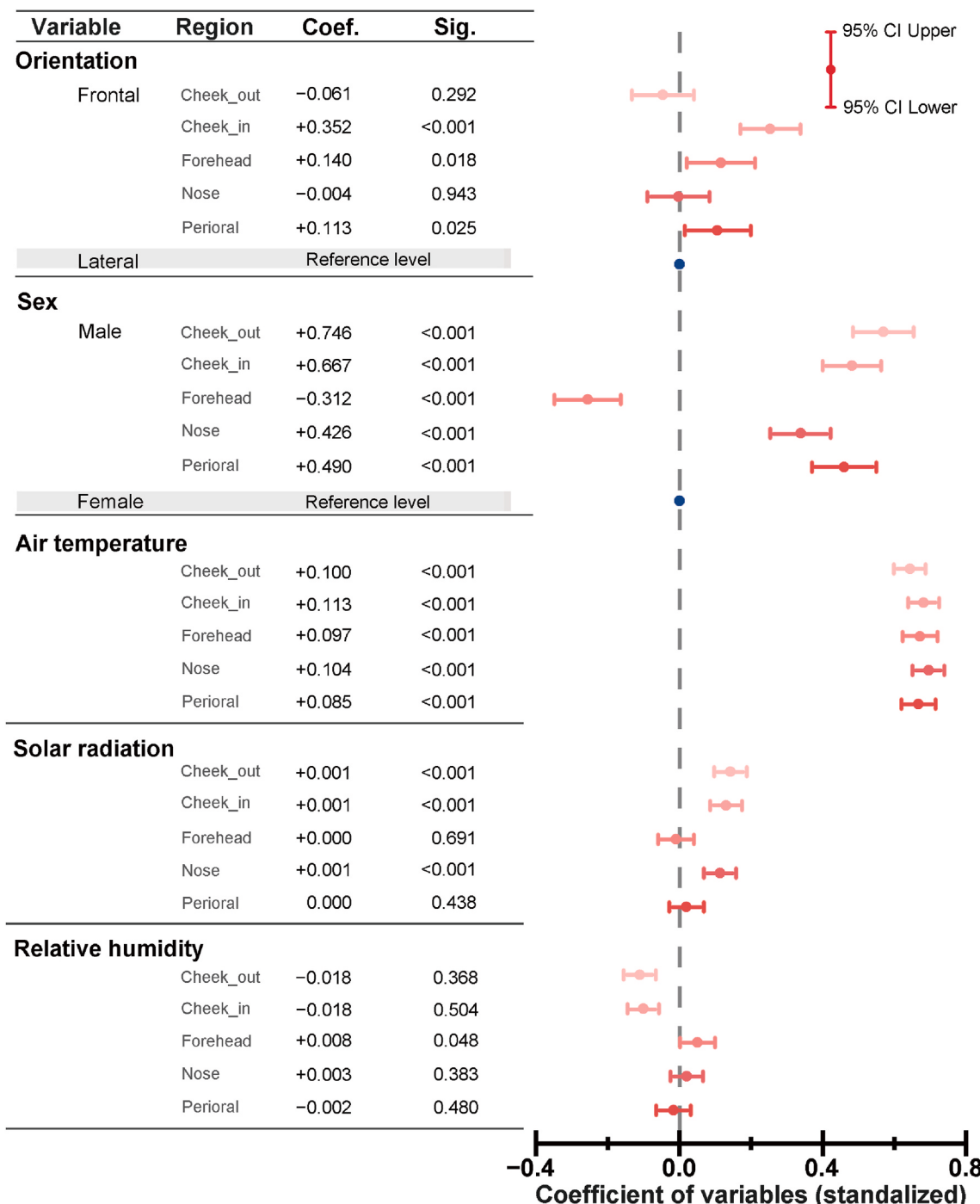


Fig. 13. Generalized linear mixed model regression results of facial skin temperature of the occupants in relation to various factors.

across the cheeks may be attributed to the right cheek not receiving direct shortwave solar radiation when the cabin was subjected to lateral solar radiation, primarily because of the cooling effect of the air temperature. Additionally, males exhibited statistically significant positive coefficients in most facial regions, indicating higher facial skin temperatures than those of females (i.e., the reference category) under identical environmental conditions. A commonly accepted explanation for the observed sex differences in skin temperature is that males have a higher basal metabolic rate, which generates more heat [50]. Regarding the forehead skin temperature, the coefficients showed that females surpassed males. This may be associated with height differences. A regression analysis was performed on the forehead skin temperatures of the participants at the 40th minute under nighttime conditions in

relation to their heights. The results revealed a significant negative correlation between height and forehead skin temperature ($R = -0.502$; $P < 0.01$). This can be attributed to the experimental setup, wherein air vents were oriented horizontally upward at a 75° angle to minimize direct airflow to the faces of the participants. However, taller participants may still be subjected to airflow from the vents, resulting in lower forehead skin temperatures. Given that males are on average taller, their foreheads may be more susceptible to the effects of airflow, potentially leading to lower forehead skin temperatures than those of females.

Further analysis of the relationship between changes in environmental parameters and skin temperature of different facial areas was conducted using multiple regression models. The results are presented in Table 5. For males, changes in cheek and nose skin temperatures are

Table 5

Multivariate regression results of facial skin temperature variations with solar radiation, air temperature, and relative humidity variations.

Sex	Dependent variable	Independent variables	Coefficients		Sig.
			Unstandardized	Standardized	
Male	$\Delta T_{\text{Cheek_out}}$	ΔSR	0.000	+0.067	0.111
		$\Delta T_{\text{air},1.1m}$	+0.057	+0.472	0.000**
		ΔRH	+0.017	+0.196	0.000**
	$\Delta T_{\text{Cheek_in}}$	ΔSR	0.000	+0.042	0.297
		$\Delta T_{\text{air},1.1m}$	+0.060	+0.485	0.000**
		ΔRH	+0.022	+0.248	0.000**
	$\Delta T_{\text{Forehead}}$	ΔSR	-0.001	-0.027	0.582
		$\Delta T_{\text{air},1.1m}$	+0.040	+0.077	0.121
		ΔRH	+0.069	+0.182	0.000**
	ΔT_{Nose}	ΔSR	0.000	-0.014	0.768
		$\Delta T_{\text{air},1.1m}$	+0.055	+0.105	0.031*
		ΔRH	+0.079	+0.208	0.000**
	$\Delta T_{\text{Perioral}}$	ΔSR	0.000	-0.007	0.881
		$\Delta T_{\text{air},1.1m}$	+0.031	+0.061	0.222
		ΔRH	+0.060	+0.161	0.001**
Female	$\Delta T_{\text{Cheek_out}}$	ΔSR	+0.001	+0.100	0.039
		$\Delta T_{\text{air},1.1m}$	+0.047	+0.325	0.000**
		ΔRH	+0.009	+0.104	0.033*
	$\Delta T_{\text{Cheek_in}}$	ΔSR	+0.001	+0.070	0.147
		$\Delta T_{\text{air},1.1m}$	+0.052	+0.332	0.000**
		ΔRH	+0.008	+0.087	0.075
	$\Delta T_{\text{Forehead}}$	ΔSR	+0.001	+0.064	0.179
		$\Delta T_{\text{air},1.1m}$	+0.062	+0.299	0.000**
		ΔRH	+0.029	+0.230	0.000**
	ΔT_{Nose}	ΔSR	+0.001	+0.063	0.176
		$\Delta T_{\text{air},1.1m}$	+0.063	+0.342	0.000**
		ΔRH	+0.027	+0.248	0.000**
	$\Delta T_{\text{Perioral}}$	ΔSR	+0.001	+0.068	0.157
		$\Delta T_{\text{air},1.1m}$	+0.049	+0.317	0.000**
		ΔRH	+0.018	+0.195	0.000**

sensitive to changes in air temperature, indicating that cheek and nose skin temperatures changes are synchronous with air temperature changes. For females, skin temperatures across different facial areas are significantly sensitive to changes in air temperature. Notably, changes in skin temperatures of different facial areas for both males and females are synchronous with changes in relative humidity. However, the results in Fig. 13 show that relative humidity is not significantly correlated with facial skin temperature. This may be due to changes in relative humidity potentially causing immediate responses in facial skin temperature; however, the rapid drop in relative humidity following the activation of the cabin A/C weakens the correlation between the two variables. Similarly, Fig. 13 shows that solar radiation is a key factor affecting facial skin temperature, particularly that of the cheeks. However, the synchronicity analysis did not reveal significant sensitivity of facial skin temperature to changes in solar radiation. This is because solar radiation did not vary periodically over time during the experiment. For the same experimental session, the amount of solar radiation the participants were exposed to remained essentially stable. This led to an analysis of the impact of solar radiation on facial skin temperature from a dynamic time perspective, where the minimal change in solar radiation experienced by the same participant was insufficient to cause changes in facial skin temperature.

4. Discussion

4.1. Correlation between facial skin temperature and thermal sensation

The perception of temperature by the human body is achieved through cold-sensitive and thermosensitive nerve endings located beneath the skin, which transmit signals to the hypothalamus via the sympathetic nervous system [51]. The body's perception of cold and

heat can lead to the dilation and constriction of blood vessels flowing through the skin, resulting in changes in skin temperature. This establishes a correlation between skin temperature and thermal sensation. Appendix Fig. S5 depicts the correlations between facial region temperatures and thermal sensation reported by the participants in the cabin environment. Notably, both the cheek and nose skin temperatures exhibited statistically significant correlations with thermal sensation, whereas the forehead and perioral skin temperatures displayed moderately significant correlations. These findings underscore the potential utility of thermal imaging for capturing the skin temperatures in the cheek and nose regions of cabin occupants to assess thermal sensation.

4.2. Important parameters affecting thermal sensation

Exposure to high temperatures can lead to discomfort, including dizziness and sore eyes [52], posing not only health risks for occupants, but also significant safety risks for drivers. This study revealed that dynamic cooling of the cabin resulted in a significant improvement in overall thermal sensation. Specifically, occupant thermal sensation was primarily influenced by changes in air temperature during this dynamic adjustment. In this study, when a vehicle was exposed to sunlight, it was more comfortable and overall healthier for occupants to activate the A/C for 7 min before entering the cabin (i.e., once cabin air temperature dropped to 30 °C or below). Once cabin air temperature stabilizes, solar radiation intensity becomes the primary factor influencing occupant thermal sensation. Under conditions of high solar radiation intensity, a cabin air temperature of 25 °C may not fully alleviate the "hot" sensation, necessitating a lower cabin air temperature to achieve a neutral occupant thermal sensation. This study demonstrates that approximately 200 W/m² of solar radiation can lead to an increase of one thermal sensation unit, which is consistent with the findings of another

study [13]. However, Zhou et al. [6] analyzed the effect of sudden changes in solar radiation on changes in thermal sensation in experiments conducted during the transition season and observed that when the human body received a sudden radiation increase of 70 W/m^2 , there was a change of approximately one thermal sensation unit. This finding is inconsistent with the results of this study. On the one hand, Zhou et al. utilized a model input derived from a simulation software to calculate the solar radiation received by the human body surface, whereas our study collected solar radiation data transmitted through the cabin glass. The former approach may yield relatively low values owing to its consideration of the projected surface area. On the other hand, the experimental setup in this study did not simulate scenarios involving mutations. A rapid alteration in solar radiation intensity could lead to distinct variations in occupant thermal sensation, contrary to those caused by gradual change.

4.3. Non-uniformity of occupant thermal sensation

In this study, when the cabin air temperature fell within the neutral range, individuals consistently reported high local thermal sensations on their backs. Previous research has indicated that, in warm environments, employing localized cooling on the back can effectively enhance the overall thermal sensation without causing localized discomfort [53]. Therefore, combining cabin seats with localized contact cooling systems could offer an energy-efficient and effective solution for rapidly improving occupant thermal sensation under high solar radiation conditions in summer. Furthermore, our study revealed no statistically significant difference in the overall thermal sensation when sunlight was hitting the cabin directly in the front compared with hitting it sideways. However, there was a significant difference in the localized thermal sensations of the non-window-side body parts. For asymmetric environments, Zhang proposed that the overall thermal sensation could be calculated using the weighted average of local thermal sensations [54]. Although the orientation of sunlight resulted in notable variations in local thermal sensations on the non-windowed sides of the body, the local thermal sensations on the windowed sides remained consistent ($P > 0.05$) (Fig. 11). This may have reduced the differences in the overall thermal sensation to some extent.

5. Limitations

This study utilized thermography for non-contact facial skin temperature measurements. Despite obtaining more comprehensive temperature distribution information, the lower accuracy compared to contact skin temperature sensors might affect the precision of the measurements. Additionally, the study was conducted in a parked state to ensure the safety of the experiments. Zhou et al. [6] mentioned in their research that occupant thermal sensation during the driving process may undergo sudden changes owing to non-thermal environmental factors. Moreover, because driving requires a high level of attention, the metabolic rate of drivers may be higher than that when sitting still. Consequently, in actual driving scenarios, the thermal sensation of drivers may differ from that of non-drivers. The third limitation is the absence of a more in-depth investigation of the influence of solar exposure area on occupant thermal sensation. This is because this study was an outdoor experiment and there was covariance between the solar elevation angle and solar radiation, posing difficulties in simultaneously incorporating both factors within a generalized linear mixed model. The fourth limitation stems from the decision to conduct experiments in an actual car cabin environment. Outdoor experiments were conducted to capture the dynamic changes occurring under real-world conditions. However, outdoor experiments cannot achieve the same level of environmental control precision as those conducted in indoor climate chambers. Despite our efforts to minimize the impact of variations in outdoor conditions on the experimental results, these variations may still influence the comparisons between different experimental groups.

The fifth limitation lies in the absence of black globe temperature measurements. This limitation arises from the extended response time and stabilization period required by black globe thermometers. These characteristics make it difficult to accurately measure the black globe temperature within a cabin, particularly considering the highly dynamic and transient nature of the environment. Moreover, it should be noted that this study simulated real-world conditions with an initially high cabin temperature. This study focuses more on the changes in comfort during the cooling process after the air conditioning is turned on, rather than delving into heat strain or heat-related illnesses under high-temperature exposure. However, under high-temperature exposure, there is a risk of dizziness, dehydration, and other health issues [55]. For the cabin environment, these risk issues warrant further investigation. In future research, supplementing measurements with core temperature, sweating rate, and other physiological information may be beneficial for assessing heat risk to health. This will facilitate a more comprehensive understanding of the thermal responses of occupants in the cabin environment.

6. Conclusions

This study was conducted in a cabin parked outdoors to investigate the impact of actual outdoor conditions on occupant thermal response and its synchronicity with environmental changes. The findings provide key optimization parameters for designing comfortable cabin thermal environments and support the feasibility of an automatic air-conditioning control system based on thermal imaging technology. The conclusions are as follows.

1. Although the initial air temperature of a cabin parked outdoors in summer is high, activating the air conditioner can quickly reduce the temperature and humidity, significantly improving the occupant thermal sensation within 7 min, with facial skin temperature and occupant thermal sensation stabilizing after 15 min.
2. Occupant thermal sensation is primarily influenced by air temperature, followed by solar radiation, and changes synchronously with both. Within a 40-min experimental period, when the air temperature stabilizes at around 26°C , approximately 200 W/m^2 of solar radiation can increase the thermal sensation by one unit.
3. The skin temperatures of the cheeks and nose are significantly affected by air temperature and solar radiation, and their changes synchronize with those of the air temperature and relative humidity.
4. Facial skin temperature is significantly correlated with occupant thermal sensation, making it theoretically feasible to use thermal imaging to monitor the facial skin temperatures of the occupants to automate air-conditioning adjustments.

CRediT authorship contribution statement

Junmeng Lyu: Writing – original draft, Visualization, Methodology, Formal analysis, Data curation, Conceptualization. **Yuxin Yang:** Writing – review & editing, Methodology. **Dayi Lai:** Writing – review & editing. **Li Lan:** Writing – review & editing. **Zhiwei Lian:** Writing – review & editing, Funding acquisition, Conceptualization.

Declaration of competing interest

The authors declare that they have no known competing financial interests or personal relationships that could have appeared to influence the work reported in this paper.

Data availability

Data will be made available on request.

Acknowledgements

This work is supported by the National Key R&D Program of China (2022YFC3803201).

Appendix A. Supplementary data

Supplementary data to this article can be found online at <https://doi.org/10.1016/j.buildenv.2024.111727>.

References

- [1] M. De Santis, L. Silvestri, A. Forcina, Promoting electric vehicle demand in Europe: design of innovative electricity consumption simulator and subsidy strategies based on well-to-wheel analysis, *Energy Convers. Manag.* 270 (2022) 116279, <https://doi.org/10.1016/j.enconman.2022.116279>.
- [2] ISO/TS 14505-1, Ergonomics of the Thermal Environment—Evaluation of Thermal Environments in Vehicles—Part 1: Principles and Methods for Assessment of Thermal Stress., (n.d.).
- [3] ISO/TS 14505-2, Ergonomics of the Thermal Environment — Evaluation of Thermal Environments in Vehicles - Part 2: Determination of Equivalent Temperature, 2006.
- [4] ISO/TS 14505-3, Ergonomics of the Thermal Environment — Evaluation of Thermal Environments in Vehicles - Part 3: Evaluation of Thermal Comfort Using Human Subjects, 2006.
- [5] ASHRAE, ANSI/ASHRAE Standard 55-2023, Thermal Environmental Conditions for Human Occupancy, 2020.
- [6] X. Zhou, D. Lai, Q. Chen, Experimental investigation of thermal comfort in a passenger car under driving conditions, *Build. Environ.* 149 (2019) 109–119, <https://doi.org/10.1016/j.buildenv.2018.12.022>.
- [7] X. Xu, L. Zhao, Z. Yang, Field experimental investigation on human thermal comfort in vehicle cabin, in: WCX SAE World Congress Experience, SAE International, 2022, <https://doi.org/10.4271/2022-01-0195>.
- [8] X. Zhou, D. Lai, Q. Chen, Thermal sensation model for driver in a passenger car with changing solar radiation, *Build. Environ.* 183 (2020) 107219, <https://doi.org/10.1016/j.buildenv.2020.107219>.
- [9] A. Grundstein, V. Meentemeyer, J. Dowd, Maximum vehicle cabin temperatures under different meteorological conditions, *Int. J. Biometeorol.* 53 (2009) 255–261, <https://doi.org/10.1007/s00484-009-0211-x>.
- [10] P. Danca, F. Bode, A. Dogeanu, C. Croitoru, M. Sandu, A. Meslem, I. Nastase, Experimental study of thermal comfort in a vehicle cabin during the summer season, *E3S Web of Conferences* 111 (2019) 1048, <https://doi.org/10.1051/e3sconf/201911101048>.
- [11] Y. Don Guan, M.H. Hosni, B.W. Jones, T.P. Giedla, Investigation of human thermal comfort under highly transient conditions for automotive applications-Part 1: experimental design and human subject testing Implementation, *Build. Eng.* 109 (2003) 885–897. <https://www.proquest.com/scholarly-journals/investigation-human-thermal-comfort-under-highly/docview/192539219/se-2?accountid=13818>.
- [12] Y. Don Guan, M.H. Hosni, B.W. Jones, T.P. Giedla, Investigation of human thermal comfort under highly transient conditions for automotive applications-Part 2: thermal sensation modeling, *Build. Eng.* 109 (2003) 898–907. <https://www.proquest.com/scholarly-journals/investigation-human-thermal-comfort-under-highly/docview/192538953/se-2?accountid=13818>.
- [13] S.G. Hodder, K. Parsons, The effects of solar radiation on thermal comfort, *Int. J. Biometeorol.* 51 (2007) 233–250, <https://doi.org/10.1007/s00484-006-0050-y>.
- [14] T. Srivilpsophon, J. Tiansuwan, T. Kiatsiriroat, Effect of anti-solar glass film on heat transfer and mean radiant temperature inside cabin of air-conditioned vehicle, *Int. J. Ambient Energy* 28 (2007) 39–50, <https://doi.org/10.1080/01430750.2007.9675022>.
- [15] E. Arens, H. Zhang, C. Huizenga, Partial- and whole-body thermal sensation and comfort— Part I: uniform environmental conditions, *J. Therm. Biol.* 31 (2006) 53–59, <https://doi.org/10.1016/j.jtherbio.2005.11.028>.
- [16] H. Zhang, E. Arens, C. Huizenga, T. Han, Thermal sensation and comfort models for non-uniform and transient environments: Part I: local sensation of individual body parts, *Build. Environ.* 45 (2010) 380–388, <https://doi.org/10.1016/j.buildenv.2009.06.018>.
- [17] E. Arens, H. Zhang, C. Huizenga, Partial- and whole-body thermal sensation and comfort—Part II: non-uniform environmental conditions, *J. Therm. Biol.* 31 (2006) 60–66, <https://doi.org/10.1016/j.jtherbio.2005.11.027>.
- [18] H. Zhang, E. Arens, C. Huizenga, T. Han, Thermal sensation and comfort models for non-uniform and transient environments, part III: whole-body sensation and comfort, *Build. Environ.* 45 (2010) 399–410, <https://doi.org/10.1016/j.buildenv.2009.06.020>.
- [19] O. Kaynakli, M. Kilic, An investigation of thermal comfort inside an automobile during the heating period, *Appl. Ergon.* 36 (2005) 301–312, <https://doi.org/10.1016/j.apergo.2005.01.006>.
- [20] M. Kilic, S.M. Akyol, Experimental investigation of thermal comfort and air quality in an automobile cabin during the cooling period, *Heat Mass Tran.* 48 (2012) 1375–1384, <https://doi.org/10.1007/s00231-012-0988-8>.
- [21] M. Kilic, O. Kaynakli, An experimental investigation on interior thermal conditions and human body temperatures during cooling period in automobile, *Heat Mass Tran.* 47 (2011) 407–418, <https://doi.org/10.1007/s00231-010-0737-9>.
- [22] M. Kilic, S.M. Akyol, The effects of using different ventilation modes during heating periods of an automobile, *ISI BILIMI VE TEKNIGI DERGİSİ-JOURNAL OF THERMAL SCIENCE AND TECHNOLOGY* 29 (2009) 25–36.
- [23] O. Kaynakli, E. Pusat, M. Kilic, Thermal comfort during heating and cooling periods in an automobile, *Heat Mass Tran.* 41 (2005) 449–458, <https://doi.org/10.1007/s00231-004-0558-9>.
- [24] L. Qi, J. Liu, L. Zhang, Q. Wu, Study on local thermal sensation and model applicability in vehicle cabin under different driving states, *Heat Mass Tran.* 57 (2021) 41–52, <https://doi.org/10.1007/s00231-020-02933-7>.
- [25] C. Croitoru, I. Nastase, F. Bode, A. Meslem, A. Dogeanu, Thermal comfort models for indoor spaces and vehicles—current capabilities and future perspectives, *Renewable Sustainable Energy Rev.* 44 (2015) 304–318, <https://doi.org/10.1016/j.rser.2014.10.105>.
- [26] W. Li, J. Chen, F. Lan, H. Xie, Human thermal sensation and its algorithmic modelization under dynamic environmental thermal characteristics of vehicle cabin, *Indoor Air* 32 (2022) e13168, 10.1111/ina.13168.
- [27] D. Ghosh, M. Wang, E. Wolfe, K. Chen, S. Kaushik, T. Han, Energy efficient HVAC system with spot cooling in an automobile - design and CFD analysis, *SAE international journal of passenger cars, Mechanical Systems* 5 (2012) 885–903, <https://doi.org/10.4271/2012-01-0641>.
- [28] A. Alahmer, M. Omar, A.R. Mayyas, A. Qattawi, Analysis of vehicular cabins' thermal sensation and comfort state, under relative humidity and temperature control, using Berkeley and Fanger models, *Build. Environ.* 48 (2012) 146–163, <https://doi.org/10.1016/j.buildenv.2011.08.013>.
- [29] P. Danca, A. Vartires, A. Dogeanu, An overview of current methods for thermal comfort assessment in vehicle cabin, *Energy Proc.* 85 (2016) 162–169, <https://doi.org/10.1016/j.egypro.2015.12.322>.
- [30] W. Zhang, J. Chen, F. Lan, Experimental study on occupant's thermal responses under the non-uniform conditions in vehicle cabin during the heating period, *Chinese Journal of Mechanical Engineering = Ji Xie Gong Cheng Xue Bao* 27 (2014) 331–339, <https://doi.org/10.3901/CJME.2014.02.331>.
- [31] X. He, X. Zhang, R. Zhang, J. Liu, X. Huang, J. Pei, J. Cai, F. Guo, Y. Wang, More intelligent and efficient thermal environment management: a hybrid model for occupant-centric thermal comfort monitoring in vehicle cabins, *Build. Environ.* 228 (2023) 109866, <https://doi.org/10.1016/j.buildenv.2022.109866>.
- [32] S. Cho, H.J. Nam, C. Shi, C.Y. Kim, S.-H. Byun, K.-C. Agno, B.C. Lee, J. Xiao, J. Y. Sim, J.-W. Jeong, Wireless, AI-enabled wearable thermal comfort sensor for energy-efficient, human-in-the-loop control of indoor temperature, *Biosens. Bioelectron.* 223 (2023) 115018, <https://doi.org/10.1016/j.bios.2022.115018>.
- [33] Y. He, H. Zhang, E. Arens, A. Merritt, C. Huizenga, R. Levinson, A. Wang, A. Ghahramani, A. Alvarez-Suarez, Smart detection of indoor occupant thermal state via infrared thermography, computer vision, and machine learning, *Build. Environ.* 228 (2023) 109811, <https://doi.org/10.1016/j.buildenv.2022.109811>.
- [34] D. Li, C.C. Menassa, V.R. Kamat, Robust non-intrusive interpretation of occupant thermal comfort in built environments with low-cost networked thermal cameras, *Appl. Energy* 251 (2019) 113336, <https://doi.org/10.1016/j.apenergy.2019.113336>.
- [35] Y. Wu, B. Cao, Recognition and prediction of individual thermal comfort requirement based on local skin temperature, *J. Build. Eng.* 49 (2022) 104025, <https://doi.org/10.1016/j.jobe.2022.104025>.
- [36] Y. Wu, B. Cao, M. Hu, G. Lv, J. Meng, H. Zhang, Development of personal comfort model and its use in the control of air conditioner, *Energy Build.* 285 (2023) 112900, <https://doi.org/10.1016/j.enbuild.2023.112900>.
- [37] J. Lyu, H. Du, Z. Zhao, Y. Shi, B. Wang, Z. Lian, Where should the thermal image sensor of a smart A/C look?-Occupant thermal sensation model based on thermal imaging data, *Build. Environ.* 239 (2023) 110405, <https://doi.org/10.1016/j.buildenv.2023.110405>.
- [38] A. Ghahramani, G. Castro, B. Becerik-Gerber, X. Yu, Infrared thermography of human face for monitoring thermoregulation performance and estimating personal thermal comfort, *Build. Environ.* 109 (2016) 1–11, <https://doi.org/10.1016/j.buildenv.2016.09.005>.
- [39] H. Tanaka, M. Kitada, Y. Taniguchi, Y. Ohno, T. Shinagawa, Study on Car Air Conditioning System Controlled by Car Occupants Skin Temperatures Part II: Development of a New Air Conditioning System, 1992.
- [40] H. Tanaka, M. Kitada, Y. Taniguchi, Y. Ohno, T. Shinagawa, Study on Car Air Conditioning System Controlled by Car Occupants Skin Temperatures Part II: Development of a New Air Conditioning System, 1992.
- [41] L. Lan, J. Tang, P. Wargo, D.P. Wyon, Z. Lian, Cognitive performance was reduced by higher air temperature even when thermal comfort was maintained over the 24–28°C range, *Indoor Air* 32 (2022) e12916, <https://doi.org/10.1111/ina.12916>.
- [42] L. Lan, Z. Lian, Application of statistical power analysis – how to determine the right sample size in human health, comfort and productivity research, *Build. Environ.* 45 (2010) 1202–1213, <https://doi.org/10.1016/j.buildenv.2009.11.002>.
- [43] F.R. d'Ambrosio Alfano, M. Dell'isola, G. Ficco, B.I. Palella, G. Riccio, On the measurement of the mean radiant temperature by means of globes: an experimental investigation under black enclosure conditions, *Build. Environ.* 193 (2021) 107655, <https://doi.org/10.1016/j.buildenv.2021.107655>.
- [44] F.R. d'Ambrosio Alfano, G. Ficco, A. Frattolillo, B.I. Palella, G. Riccio, Mean radiant temperature measurements through small black globes under forced convection conditions, *Atmosphere* 12 (2021) 621, <https://doi.org/10.3390/atmos12050621>.

- [45] D.A. McIntyre, *Indoor Climate*, London : Applied Science Publishers, London, 1980.
- [46] Z. Hou, J. Lyu, D. Wu, J. Chen, J. Shi, Z. Lian, Occupant-centric cabin thermal sensation assessment system based on low-cost thermal imaging, *Build. Environ.* (2024) 111692, <https://doi.org/10.1016/j.buildenv.2024.111692>.
- [47] S. Karjalainen, Thermal comfort and gender: a literature review, *Indoor Air* 22 (2012) 96–109, <https://doi.org/10.1111/j.1600-0668.2011.00747.x>.
- [48] H. Du, Z. Zhao, J. Lyu, J. Li, Z. Liu, X. Li, Y. Yang, L. Lan, Z. Lian, Gender differences in thermal comfort under coupled environmental factors, *Energy Build.* 295 (2023) 113345, <https://doi.org/10.1016/j.enbuild.2023.113345>.
- [49] T. Parkinson, S. Schiavon, R. de Dear, G. Brager, Overcooling of offices reveals gender inequity in thermal comfort, *Sci. Rep.* 11 (2021) 23684, <https://doi.org/10.1038/s41598-021-03121-1>.
- [50] A. De Lorenzo, A. Tagliabue, A. Andreoli, G. Testolin, M. Comelli, P. Deurenberg, Measured and predicted resting metabolic rate in Italian males and females, aged 18–59 y, *Eur. J. Clin. Nutr.* 55 (2001) 208–214, <https://doi.org/10.1038/sj.ejcn.1601149>.
- [51] E.R. Nadel, R.W. Bullard, J.A. Stolwijk, Importance of skin temperature in the regulation of sweating, *J. Appl. Physiol.* 31 (1971) 80–87, <https://doi.org/10.1152/jappl.1971.31.1.80>.
- [52] S. Tham, R. Thompson, O. Landeg, K.A. Murray, T. Waite, Indoor temperature and health: a global systematic review, *Publ. Health* 179 (2020) 9–17, <https://doi.org/10.1016/j.puhe.2019.09.005>.
- [53] Q. Zhao, J. Lyu, H. Du, Z. Lian, Z. Zhao, Gender differences in thermal sensation and skin temperature sensitivity under local cooling, *J. Therm. Biol.* 111 (2023) 103401, <https://doi.org/10.1016/j.jtherbio.2022.103401>.
- [54] H. Zhang, *Human Thermal Sensation and Comfort in Transient and Non-uniform Thermal Environments*, University of California, Berkeley, 2003.
- [55] P. Habibi, G. Moradi, H. Dehghan, A. Moradi, A. Heydari, The impacts of climate change on occupational heat strain in outdoor workers: a systematic review, *Urban Clim.* 36 (2021) 100770, <https://doi.org/10.1016/j.uclim.2021.100770>.